Thermodynamic Geometry of Nonequilibrium Fluctuations in Cyclically Driven Transport

Zi Wang (王子) and Jie Ren (任捷)*

Center for Phononics and Thermal Energy Science, China-EU Joint Lab on Nanophononics, Shanghai Key Laboratory of Special Artificial Microstructure Materials and Technology, School of Physics Science and Engineering, Tongji University, Shanghai 200092, China

(Received 11 April 2023; revised 6 September 2023; accepted 11 April 2024; published 14 May 2024)

Nonequilibrium thermal machines under cyclic driving generally outperform steady-state counterparts. However, there is still lack of coherent understanding of versatile transport and fluctuation features under time modulations. Here, we formulate a theoretical framework of thermodynamic geometry in terms of full counting statistics of nonequilibrium driven transports. We find that, besides the conventional dynamic and adiabatic geometric curvature contributions, the generating function is also divided into an additional nonadiabatic contribution, manifested as the metric term of full counting statistics. This nonadiabatic metric generalizes recent results of thermodynamic geometry in near-equilibrium entropy production to far-from-equilibrium fluctuations of general currents. Furthermore, the framework proves geometric thermodynamic uncertainty relations of near-adiabatic thermal devices, constraining fluctuations in terms of statistical metric quantities and thermodynamic length. We exemplify the theory in experimentally accessible driving-induced quantum chiral transport and Brownian heat pump.

DOI: 10.1103/PhysRevLett.132.207101

Introduction.—In the past decade, significant advances have been achieved in both experiments and theories that allow for direct manipulations of thermodynamics of small setups [1–9]. These systems are subject to large fluctuations that are detrimental to their stable output. Recently, it has been shown that cyclically driven thermal devices can be tuned to be more stable and perform better than their steady-state counterparts [10–12], igniting a surge of interest into the stochastic thermodynamics of this regime.

The concept of geometry provides deep insights into the nonequilibrium cyclic driving. Its manifestation in transport was originally introduced in the Thouless pump, relating the quantization of pumped charge with the overall integral of the underlying nontrivial Berry curvature [13,14]. This idea also generalizes to open systems [15–17]. In thermal devices, the geometric-phase-like contribution provides a way of directing heat flow [18–27] and constructing heat engines [28–31] and thermoelectric pumps [32]. These geometric results, ranging from quantum Markovian systems [18] to classical diffusive dynamics [27], were mainly restricted to the adiabatic slow driving protocols. By utilizing controls, nonadiabatic pump effect can be eliminated at the expense of extra dissipations [33,34]. The leading order nonadiabatic dissipation in the finite but small driving frequency regime [35] is captured by the concept of thermodynamic metric [36–39]. Yet, in the arbitrarily fast regime, the average entropy production assumes another geometric interpretation that is lower bounded by the Wasserstein distance [40–43], providing insights into the optimal control of the dissipation during finite-time processes [44–46]. The above thermodynamic metric structures, defined on the probability manifold, make the derivation of efficiency-power trade-off [31,47–49] and the optimal protocol design [50–62] straightforward.

However, previous nonadiabatic results based on the metric structure are merely restricted to the analysis of average work or entropy production without temperature bias. This leads to little understanding of the generic transport behaviors in open systems with nonequilibrium reservoirs, let alone the transport fluctuations thereof. Therefore, important questions arise naturally. How does one analyze general currents and fluctuations in nonadiabatic cyclic thermal devices? Can the nonadiabatic driven transport be characterized by a nonequilibrium thermodynamic metric structure? If so, what are the general constraints on transport fluctuations caused thereby?

In this Letter, we solve the problems by formulating a geometric scheme of the generating function of currents, representing the nonadiabatic effects on each order of current cumulants as a metric term of full counting statistics. Based on this statistical metric structure of nonequilibrium transport, we then derive geometric thermodynamic uncertainty relations (geometric TURs) to constrain the current fluctuations under the near-adiabatic driving in terms of statistical metric quantities and thermodynamic length. Originally, the TUR was proposed [63] and proved theoretically [64,65] and experimentally [66,67] within the steady states of classical Markovian dynamics, which bounds the precision of fluctuating current Q in terms of the entropy production. The TUR was subsequently generalized to the finite-time regime [68–70], quantum systems endowed with coherence effects [71–73], setups with broken time-reversal symmetry [74,75], and even systems with feedback controls [69,76]. Also, the well established fluctuation theorems [77,78] prove the fluctuation theorem uncertainty relations [79]. For reviews on TUR, see Ref. [80]; for subsequent applications to the thermodynamic inference, see Refs. [81–83]. Importantly, Koyuk, Seifert, and Pietzonka have derived a set of modified TURs, applicable to driven systems, by taking into account the dependence of currents on the driving frequency [84–86].

Our results in this Letter advance the understanding of nonadiabatic geometric effects in parametrically driven thermal devices, which can be far from equilibrium. This allows for a study of fluctuating devices with various thermal functionalities regarding both average performance and fluctuation strength, paving the way toward designing precise thermal devices under nonequilibrium reservoirs and nonadiabatic cyclic modulations.

Setups.—We consider a cyclically driven open system coupled to multiple reservoirs B_ν, which is schematically shown in Fig. 1(a). The protocol parametrized as $\mathbf{\Lambda}(t+\tau_{\mathrm{p}})=\mathbf{\Lambda}(t)$ forms a closed curve $\partial\Omega$ in the parameter space $\mathbf{\Lambda}$, with τ_{p} being the driving period. Without loss of generality, we here take the discrete state case as an example. Similar discussions also apply for continuous cases. As such, the system distribution function is $|p(t)\rangle \coloneqq (p_1,\ldots,p_N)^{\mathrm{T}}$, with $p_i (1\le i\le N)$ describing the probability of occupying state i. The transition rate along $j\to i$ induced by the νth reservoir is k_{ij}^{ν} $(i\neq j)$, which can be time dependent under the protocol $\mathbf{\Lambda}(t)$. The master equation is thus written as $\partial_t|p(t)\rangle=\hat{L}(t)|p(t)\rangle$ with $L_{ij}=\sum_\nu(k_{ij}^{\nu}-\delta_{ij}\sum_{l\neq i}k_{li}^{\nu})$ conserving the probability during transitions by $\sum_i L_{ij}=0$.

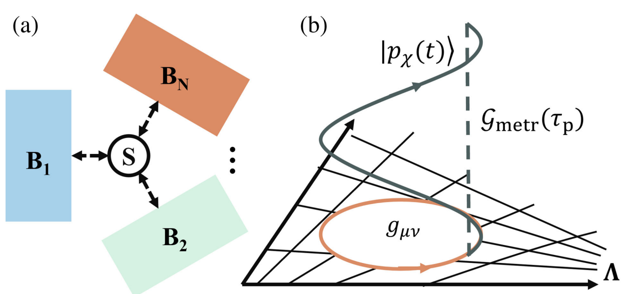

FIG. 1. Metric geometry in cyclically driven transport. (a) Nonequilibrium cyclically driven system S coupled to multiple reservoirs B_ν $(\nu=1,2,\ldots,N)$. (b) Metric structure of the cumulant generating function (CGF) $\mathcal{G}_{\mathrm{metr}}(\tau_{\mathrm{p}})=\int_0^{\tau_{\mathrm{p}}}dtg_{\mu\nu}\dot{\Lambda}_\mu\dot{\Lambda}_\nu$ in the curved parameter space $\mathbf{\Lambda}$. The dashed line represents a metric CGF contribution $\mathcal{G}_{\mathrm{metr}}(t)$ to the twisted distribution $|p_\chi(t)\rangle$ and describes the fluctuations in the nonadiabatic regime with an arbitrary driving speed, with χ being an auxiliary counting parameter for the interested current.

To each transition path k_{ij}^{ν}, we associate an increment of the accumulated current $\Delta Q=d_{ij}^{\nu}$ [80]. Stochastic exchanges between the system and reservoirs, like the current of particle number, heat, or work, are described by the antisymmetric tensor $d_{ij}^{\nu}=-d_{ji}^{\nu}$. While, the symmetric counterpart $d_{ij}^{\nu}=d_{ji}^{\nu}$ corresponds to time-reversal invariant quantities like dynamic activity ($d_{ij}^{\nu}=1$) [87]. The evolution of the full counting statistics of accumulated currents can be considered by the twisted operator $\hat{L}_\chi$ with the counting field χ:

$$\partial_t|p_\chi(t)\rangle=\hat{L}_\chi(t)|p_\chi(t)\rangle, \tag{1}$$

where the matrix elements are $L_{\chi,ij}=\sum_\nu k_{ij}^{\nu}e^{\chi d_{ij}^{\nu}}$ for $i\neq j$ and $L_{\chi,ii}=L_{ii}$. By defining the cumulant generating function (CGF) $\mathcal{G}\coloneqq\ln\mathcal{Z}=\ln\langle 1|p_\chi(t)\rangle$, the nth cumulant of stochastic accumulated current Q at time t is obtained by taking the n-order derivative of CGF with respect to χ, as $\langle Q^n\rangle_{\mathrm{c}}=\partial_\chi^n\mathcal{G}|_{\chi=0}$. Here, $\langle 1|$ is a vector with all elements being 1 and $\mathcal{Z}$ is the moment generating function encoding each order of moments by $\langle Q^n\rangle=\partial_\chi^n\mathcal{Z}|_{\chi=0}$. The non-Hermitian $\hat{L}_\chi$ can be decomposed into $\hat{L}_\chi=\sum_{n=0}^{N}E_n|r_n\rangle\langle l_n|$, where the left and right eigenvectors are biorthogonal $\langle l_m|r_n\rangle=\delta_{m,n}$ and $n=0$ corresponds to the unique steady state (we assume the ground state of $\hat{L}_\chi$ is nondegenerate). For details of the dynamics of the twisted master equation, see Sec. I of [88].

Thermodynamic geometry of full counting statistics.—Here, we sketch the derivation scheme of our most general geometric formulation. For derivation details, see Sec. II of [88]. After several driving cycles, the system enters its cyclic state, satisfying the Floquet theorem

$$|p_\chi(t)\rangle=e^{\mathcal{G}(t)}|\phi(t)\rangle=e^{\mathcal{G}_{\mathrm{dyn}}(t)+\mathcal{G}_{\mathrm{geo}}(t)}|\phi(t)\rangle, \tag{2}$$

where $|\phi(t+\tau_{\mathrm{p}})\rangle=|\phi(t)\rangle$ is a cyclic state and $|p_\chi(t)\rangle$ only accumulates a CGF $\mathcal{G}(\tau_{\mathrm{p}})=\mathcal{G}_{\mathrm{dyn}}(\tau_{\mathrm{p}})+\mathcal{G}_{\mathrm{geo}}(\tau_{\mathrm{p}})$ during one driving period. It shows clearly that in addition to the dynamic-phase-like steady states contribution $\mathcal{G}_{\mathrm{dyn}}(\tau_{\mathrm{p}})\coloneqq\int_0^{\tau_{\mathrm{p}}}dtE_0(t)$, there is a general geometric contribution,

$$\mathcal{G}_{\mathrm{geo}}(\tau_{\mathrm{p}})=-\oint_{\partial\Omega}d\Lambda_\mu\langle l_0|\partial_\mu\phi(t)\rangle, \tag{3}$$

where we define $\partial_\mu\coloneqq\partial_{\Lambda_\mu}$ for short. $\mathcal{G}_{\mathrm{geo}}$ is formally analogous to the Aharonov-Anandan phase in driven quantum systems [90], containing both the adiabatic and nonadiabatic effects. $\mathcal{G}_{\mathrm{dyn}}$ is simply an average over instantaneous steady states, while $\mathcal{G}_{\mathrm{geo}}$ has no static analogs. Specifically, one can decompose the state $|\phi\rangle$ into the adiabatic and nonadiabatic components, which are respectively the instantaneous steady state $|r_0\rangle$ and the transverse states perpendicular to $|r_0\rangle$ as

$$|\phi(t)\rangle = |r_0(t)\rangle + \hat{G}|\partial_t\phi(t)\rangle, \tag{4}$$

where the operator $\hat{G} := (\hat{L}_\chi - E_0)^+(\hat{1} - |\phi\rangle\langle l_0|)$, with the pseudoinverse $(\hat{L}_\chi - E_0)^+ = \sum_{n\neq 0}[1/(E_n - E_0)]|r_n\rangle\langle l_n|$. The first term is the adiabatic trajectory and the second term signifies the nonadiabatic excitations.

By substituting Eq. (4) into Eq. (3), we find that the geometric CGF is generally divided into two parts: $\mathcal{G}_{\rm geo} = \mathcal{G}_{\rm curv} + \mathcal{G}_{\rm metr}$. The first part is the adiabatic Berry-curvature-like CGF $\mathcal{G}_{\rm curv} = \oint_{\partial\Omega} d\Lambda_\mu A_\mu = \int_\Omega dS_{\mu\nu}F_{\mu\nu}$ [18,24,27–30] with the geometric connection $A_\mu = -\langle l_0|\partial_\mu r_0\rangle$ and the antisymmetric curvature $F_{\mu\nu} = \langle\partial_\nu l_0|\partial_\mu r_0\rangle - \langle\partial_\mu l_0|\partial_\nu r_0\rangle$, governing the current statistics in the adiabatic regime. This regime is fertile in constructing precise and efficient adiabatic thermal machines [9–12].

Of our prime interest is actually the second part, the nonadiabatic metric component

$$\mathcal{G}_{\rm metr}(\tau_{\rm p}) = \int_0^{\tau_{\rm p}} g_{\mu\nu}\dot{\Lambda}_\mu\dot{\Lambda}_\nu dt,$$
$$\text{with}\quad g_{\mu\nu} := \frac{1}{2}\left[\langle\partial_\mu l_0|\hat{G}|\partial_\nu\phi\rangle + \langle\partial_\nu l_0|\hat{G}|\partial_\mu\phi\rangle\right], \tag{5}$$

from which the full nonadiabatic effect on each order of fluctuation cumulants can be derived $\langle Q^n_{\rm metr}\rangle_{\rm c} := \partial^n_\chi\mathcal{G}_{\rm metr}|_{\chi=0} = \int_0^{\tau_{\rm p}} g^{Q^n}_{\mu\nu}\dot{\Lambda}_\mu\dot{\Lambda}_\nu dt$, with the corresponding metric for cumulants being $g^{Q^n}_{\mu\nu} := \partial^n_\chi g_{\mu\nu}|_{\chi=0}$. This metric structure in CGF is illustrated in Fig. 1(b). In contrast to the time-antisymmetric $\mathcal{G}_{\rm curv}$ that reverses upon time reversal, the time-symmetric metric tensor (also symmetric in the sense of $g_{\mu\nu} = g_{\nu\mu}$) indicates that the nonadiabatic component $\mathcal{G}_{\rm metr}$ provides a time-reversal invariant contribution of each current and the corresponding fluctuations. We note that although Eq. (5) is merely a formal solution, the following concrete results follow from it.

The statistical metric Eq. (5) describes the full nonadiabatic effect on arbitrary transport fluctuations. In the near-adiabatic regime, the state $|\phi(t)\rangle$ reduces to $|r_0(t)\rangle$ and the metric simplifies to the leading order of nonadiabaticity as

$$\mathfrak{g}_{\mu\nu} = \sum_{n\neq 0}\frac{\langle\partial_\mu l_0|r_n\rangle\langle l_n|\partial_\nu r_0\rangle + (\mu\leftrightarrow\nu)}{2(E_n - E_0)}, \tag{6}$$

which describes the near-adiabatic currents and fluctuations. Here, $(\mu\leftrightarrow\nu)$ means interchanging indices. Previous works on the thermodynamic geometry can be derived by restricting to this near-equilibrium regime and considering only the average entropy production [37,39,48] and work variance [52] in setups with a single equilibrium reservoir.

It is worth noting that, in the geometry of optimal transport, the cost of changing between distributions, i.e., the average entropy production, is determined by other metrics on the probability manifold [41–43], both for the overdamped [40,44], underdamped Brownian [46], and discrete master equation case [43,45]. The minimization of average entropy production naturally reduces to finding the geodesic between initial and final distributions, whose length is bounded from below by the Wasserstein distance [40,43], leading to the optimal Landauer erasure [40,54,62]. Distinct from the above regime, the metric Eq. (5) here works in the geometry of parameter space, which is valid for any currents and fluctuations of interest under cyclic parametric driving. In what follows, we will discuss implications of the statistical metric of CGF on average currents and fluctuations, separately.

Metric structure and average currents.—Here, we consider consequences of the CGF metric on the average current. Details of calculation are summarized in Sec. III of [88]. We show that the average current during one period is $\langle Q\rangle := \partial_\chi\mathcal{G}(\tau_{\rm p})|_{\chi=0} = \int_0^{\tau_{\rm p}} dt\langle 1|\hat{J}(t)|p(t)\rangle$, with the current operator being $\hat{J} := \partial_\chi\hat{L}_\chi|_{\chi=0}$ and the cyclic distribution being $|p(t)\rangle = |p_\chi(t)\rangle|_{\chi=0}$. Particularly, we derive the nonadiabatic metric structure for current Q as

$$\langle Q_{\rm metr}\rangle := \partial_\chi\mathcal{G}_{\rm metr}(\tau_{\rm p})|_{\chi=0} = \int_0^{\tau_{\rm p}} g^Q_{\mu\nu}\dot{\Lambda}_\mu\dot{\Lambda}_\nu dt,$$
$$\text{with}\quad g^Q_{\mu\nu} = \frac{1}{2}\left[\langle 1|\hat{J}\hat{L}^+\partial_\mu(\hat{L}^+|\partial_\nu p\rangle) + (\mu\leftrightarrow\nu)\right], \tag{7}$$

where $g^Q_{\mu\nu} = \partial_\chi g_{\mu\nu}|_{\chi=0}$ is a symmetric metric with respect to the average accumulated current $\langle Q\rangle$ and $\hat{L}^+$ is the pseudoinverse of $\hat{L}_\chi|_{\chi=0}$. It is worth noting that Eq. (7) works for arbitrary nonadiabatic driving speed. If one replaces $|p\rangle$ by the instantaneous steady states $|\pi\rangle = |r_0\rangle|_{\chi=0}$ in Eq. (7), one will enter in the near-adiabatic regime and obtain the corresponding metric $\mathfrak{g}^Q_{\mu\nu} = \left[\langle 1|\hat{J}\hat{L}^+\partial_\mu(\hat{L}^+|\partial_\nu\pi\rangle) + (\mu\leftrightarrow\nu)\right]/2$, which describes the leading order finite-time effect.

Here, we discuss the application of Eq. (7) to thermodynamic optimization. In the instantaneously unbiased case, the metric of total entropy production can be expressed as $\tilde{g}_{tt} = g^\Sigma_{tt} + \partial_t(\sigma_p - \sigma_\pi)$, where time-dependent metric g^Σ_{tt} describes the reservoir entropy production due to heat currents and $\partial_t(\sigma_p - \sigma_\pi)$ is the system entropy production rate, with $\sigma_p = -\sum_n p_n \ln p_n$. Note that over one whole period, $\langle\Sigma\rangle := \int_0^{\tau_{\rm p}} dt g^\Sigma_{tt} = \int_0^{\tau_{\rm p}} dt\tilde{g}_{tt}$ since $|p\rangle$ and $|\pi\rangle$ is cyclic in time. The positivity of total entropy production guarantees $\tilde{g}_{tt} > 0$, which allows us to obtain a thermodynamic speed limit $\tau_{\rm p} \geq \mathcal{L}^2/\langle\Sigma\rangle$, bounding the system evolution speed with entropy production and nonequilibrium thermodynamic length $\mathcal{L} = \int_0^{\tau_{\rm p}} dt\sqrt{\tilde{g}_{tt}}$. The sign of equality is obtained when the entropy production rate is constant and this endows us an entropy minimization principle $\partial_t\tilde{g}_{tt} = 0$.

We note that the pseudo-Riemannian metric $g^Q_{\mu\nu}$ is not promised to be positive-definite. Nevertheless, this "nonpositive definiteness" sacrifice allows us to generalize the previous thermodynamic geometry framework to nonequilibrium transports for generic currents in finite-time driving regimes. For example, in the near-adiabatic regime, we can obtain the vector field in the parameter space along which the nonadiabatic pump current vanishes $\mathfrak{g}^{Q}_{\mu\nu}\dot{\Lambda}^{\mu}\dot{\Lambda}^{\nu}=0$. This provides us a geometric view point of the nonadiabatic control over the time-dependent pump effect. For details of this optimization principle, see Sec. IV of [88]. The concise average current expression Eq. (7) is simply a consequence of our general result Eq. (5), which generally encodes the statistical information of each order fluctuation cumulants $\langle Q^{n}_{\mathrm{metr}}\rangle_{\mathrm{c}}$.

Geometric TURs and fluctuations.—Here, by restricting to the near-adiabatic regime, we show that the fluctuations encoded by Eq. (6) are constrained by a kind of geometric TURs, wherein the two geometric terms originated from $\mathcal{G}_{\mathrm{geo}}=\mathcal{G}_{\mathrm{curv}}+\mathcal{G}_{\mathrm{metr}}$ play a central role. Based on the fluctuation-response inequality [89], which is a nonlinear generalization of the Cramer-Rao bound, we obtain the geometric TURs (see Sec. V of [88] for details) as

$$\langle\Sigma\rangle\geq 2\frac{(\langle Q_{\mathrm{dyn}}\rangle-\langle Q_{\mathrm{metr}}\rangle)^{2}}{\langle Q^{2}\rangle_{\mathrm{c}}}\coloneqq\Sigma_{\mathrm{g}},\qquad(8)$$

where Σ is the entropy production during one driving period, Q_{dyn} and Q_{metr} are respectively the dynamic and nonadiabatic metric components of an arbitrary current with $d^{\nu}_{ij}=-d^{\nu}_{ji}$ (that can be particle number, heat, or work). Both the variance $\langle Q^{2}\rangle_{\mathrm{c}}$ and entropy production $\langle\Sigma\rangle$ contain separate contributions of the dynamic, adiabatic curvature, and nonadiabatic metric origins. Equation (8), consistent with Ref. [85], generalizes the adiabatic limit results in a thermoelectric heat engine [91]. It clearly unveils the role played by the near-adiabatic metric structure and paves the way toward geometric inference and optimization.

Now let us show some direct consequences of the geometric TURs on the near-adiabatic but finite-time processes. If the reservoirs are instantaneously isothermal with each other, the dynamic components vanish in the sense of mean values $\langle Q_{\mathrm{dyn}}\rangle=\langle\Sigma_{\mathrm{dyn}}\rangle=0$, but not necessarily for the fluctuation $\langle Q^{2}_{\mathrm{dyn}}\rangle_{\mathrm{c}}$ of an arbitrary current. Meanwhile, $\langle\Sigma_{\mathrm{curv}}\rangle=0$ due to the vanishing quasistatic entropy production. By rewriting Eq. (8) as $\langle Q^{2}\rangle_{\mathrm{c}}\geq 2(\langle Q_{\mathrm{dyn}}\rangle-\langle Q_{\mathrm{metr}}\rangle)^{2}/(\langle\Sigma_{\mathrm{dyn}}\rangle+\langle\Sigma_{\mathrm{curv}}\rangle+\langle\Sigma_{\mathrm{metr}}\rangle)$, we can obtain a geometric bound for the current fluctuation

$$\langle Q^{2}\rangle_{\mathrm{c}}\geq 2\frac{\langle Q_{\mathrm{metr}}\rangle^{2}}{\langle\Sigma_{\mathrm{metr}}\rangle},\qquad(9)$$

which becomes tighter for faster drivings. By taking the entropy production as the current ($Q\coloneqq\Sigma$) and considering the positive definiteness of $\mathfrak{g}^{\Sigma}_{\mu\nu}$, we can bound the fluctuation of entropy production Σ by the thermodynamic length $\mathcal{L}$ as

$$\langle\Sigma^{2}\rangle_{\mathrm{c}}\geq\frac{2\mathcal{L}^{2}}{\tau_{\mathrm{p}}},\qquad(10)$$

where $\mathcal{L}\coloneqq\oint_{\partial\Omega}\sqrt{\mathfrak{g}^{\Sigma}_{\mu\nu}d\Lambda_{\mu}d\Lambda_{\nu}}$ is a geometric quantity independent of the parametrization of protocol. Here, we have used both Eq. (9) and the Cauchy-Schwarz inequality [37,48]: $\langle\Sigma^{2}\rangle_{\mathrm{c}}\geq 2\langle\Sigma_{\mathrm{metr}}\rangle=2\int_{0}^{\tau_{\mathrm{p}}}\mathfrak{g}^{\Sigma}_{\mu\nu}\dot{\Lambda}_{\mu}\dot{\Lambda}_{\nu}dt\geq 2\mathcal{L}^{2}/\tau_{\mathrm{p}}$. This result can be understood as a kind of fluctuation-dissipation inequality. The geometric bound Eq. (10) connects the entropy production fluctuation in near-equilibrium finite-time processes to previously defined thermodynamic length [36,37], providing a basis for inferring the statistical distribution of entropy production in cyclically driven processes.

In the following, we will validate the metric structure Eq. (6) and the geometric TURs [Eqs. (8) and (10)] using two examples.

Discrete master equation system.—Our first model is the nonequilibrium quantum tricycle generating the chiral current by the cyclic driving, illustrated in Fig. 2(a), which is inspired by the classical stochastic pump model [17,92] and steady-state continuous thermal devices [93].

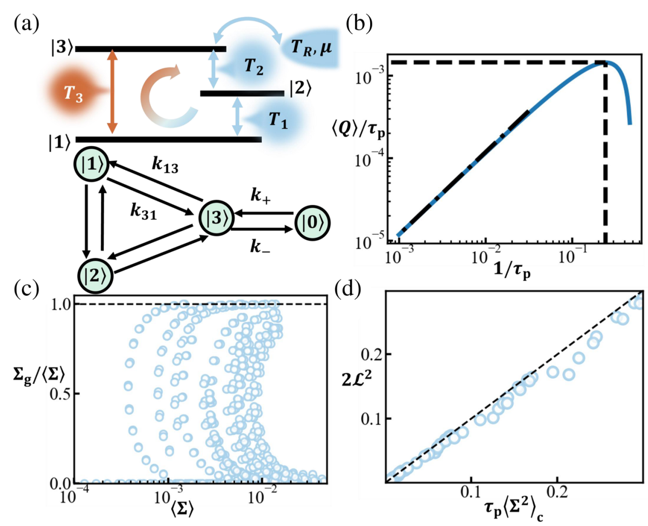

FIG. 2. Nonequilibrium quantum tricycle model with energy levels ϵ_n of quantum dots being driven. (a) The system setup and its transition graph. Three quantum dots with tunable energy levels are mediated by three thermal photonic or phononic reservoirs. The level $|3\rangle$ is in addition coupled to an electron reservoir. (b) The nonadiabatic average heat flux versus the inverse period ($\phi=2\pi/3$ and $T_1=T_2=T_3=T_R$). The dot-dash line is for the adiabatic component and the dash line is for the optimal period. (c) The geometric TUR [$\Sigma_{\mathrm{g}}\coloneqq 2(\langle Q_{\mathrm{dyn}}\rangle-\langle Q_{\mathrm{metr}}\rangle)^{2}/\langle Q^{2}\rangle_{c}$] is verified. (d) The geometric bound on the fluctuation of entropy production $\langle\Sigma^{2}\rangle_{\mathrm{c}}\tau_{\mathrm{p}}\geq 2\mathcal{L}^{2}$ is verified.

The system Hamiltonian $\hat{H} = \hat{H}_S + \hat{H}_R + \hat{H}_{SR} + \hat{H}_B + \hat{H}_{SB}$ is composed of the three quantum dot levels $\hat{H}_S = \sum_{n=1}^{3} \epsilon_n \hat{c}_n^\dagger \hat{c}_n$, the electron reservoirs $\hat{H}_R = \sum_k \epsilon_k \hat{d}_k^\dagger \hat{d}_k$, the tunneling term $\hat{H}_{SR} = \sum_k t_k (\hat{d}_k^\dagger \hat{c}_3 + \hat{c}_3^\dagger \hat{d}_k)$, the Bosonic thermal reservoir $\hat{H}_B = \sum_{\nu=1;k}^{\nu=3} \epsilon_{\nu,k} \hat{a}_{\nu,k}^\dagger \hat{a}_{\nu,k}$, and the system-reservoir coupling term $\hat{H}_{SB} = \sum_{\nu=1;k}^{\nu=3} r_{\nu,k} (\hat{a}_{\nu,k} + \hat{a}_{\nu,k}^\dagger)(\hat{c}_\nu^\dagger \hat{c}_{\nu+1} + \hat{c}_{\nu+1}^\dagger \hat{c}_\nu)$. Here, $\nu = 4$ denotes the same site as $\nu = 1$. $\hat{H}_{SB}$ mediates the transitions between quantum dots $|i\rangle$ and $|i+1\rangle$ $(1 \leq i \leq 3)$ and $\hat{H}_{SR}$ enables electrons to hop into (out of) the system through the transition $|0\rangle \to |3\rangle$ $(|3\rangle \to |0\rangle)$. We restrict ourselves to the Coulomb blockade and the weak coupling regime. For the twisted master equation and driving protocols, see Sec. VIA in [88].

By driving the energy level of quantum dots ϵ_n out of phase, e.g., $\epsilon_n(t) = \epsilon_n^0 + \delta \sin[2\pi t/\tau_\mathrm{p} + (n-1)\phi]$ with δ being the driving amplitude, we realize the driving-induced chiral current even in the absence of biases. As shown in Fig. 2(b), $\langle Q\rangle/\tau_\mathrm{p}$ is decreased by the nonadiabatic effect and reaches its maximum $-\langle Q_\mathrm{curv}\rangle^2/(4\tau_\mathrm{p}\langle Q_\mathrm{metr}\rangle)$ at the optimal period $-2\tau_\mathrm{p}\langle Q_\mathrm{metr}\rangle/\langle Q_\mathrm{curv}\rangle$ as denoted by the dashed lines. In contrast to the nonzero pumping here in quantum regime, by merely driving the energy level (the well depth) of the classical analog satisfying the Arrhenius law of transition rates, the chiral current is prohibited by the no-pumping theorem in classical systems [17,94]. As shown in Fig. 2(c), the average entropy production can be bounded and inferred by the chiral current fluctuations, satisfying Eq. (8). Also, as shown in Fig. 2(d), the fluctuation of the entropy production itself is bounded from left by the thermodynamic length, validating the geometric bound Eq. (10).

Continuous Brownian system.—Here, we show that Eq. (10) can be saturated in a Brownian heat pump engine. We consider two linearly coupled harmonic oscillators between two reservoirs of temperature T_i [19]. The Langevin dynamics is $\Gamma\dot{\mathbf{x}} = K\mathbf{x} + \boldsymbol{\xi}(t)$, where $\mathbf{x} = (x_1, x_2)^\mathrm{T}$ is the oscillators' position and $\boldsymbol{\xi} = (\xi_1, \xi_2)^\mathrm{T}$ is a vector of independent Gaussian white noise satisfying $\langle \xi_i\rangle = 0$, $\langle \xi_i(t_1)\xi_j(t_2)\rangle = 2\gamma_i T_i \delta_{ij}\delta(t_1 - t_2)$. The viscosity and stiffness matrices are $\Gamma = \left(\begin{smallmatrix}\gamma_1, 0\\ 0, \gamma_2\end{smallmatrix}\right)$, $K = k\left(\begin{smallmatrix}-1, 1\\ 1, -1\end{smallmatrix}\right)$.

By analytical calculation, when $\boldsymbol{\Lambda} = (k, \gamma_1)^\mathrm{T}$ is driven, the metric for the average entropy production $\mathfrak{g}_{\mu\nu}^{\Sigma}$ and entropy variance $\mathfrak{g}_{\mu\nu}^{\Sigma^2}$ in the isothermal case $(T_1 = T_2)$ satisfies $\mathfrak{g}_{\mu\nu}^{\Sigma^2} = 2\mathfrak{g}_{\mu\nu}^{\Sigma}$. Our bound Eq. (10) is saturable by reparametrizing the protocol in terms of the thermodynamic length, i.e., the time spent around a parameter point being $dt = (\tau_\mathrm{p}/\mathcal{L})\sqrt{\mathfrak{g}_{\mu\nu}^{\Sigma} d\Lambda_\mu d\Lambda_\nu}$ [37,48]. For details, see the Sec. VIB of [88].

Summary.—We have proposed a general framework of *nonequilibrium thermodynamic geometry* in terms of full counting statistics for analyzing the transport fluctuations in cyclically driven systems. Our theory can study the fluctuation properties of arbitrary currents among multiple reservoirs under finite-time modulations. As an illustration, we have proved and validated the geometric TURs, relating the current fluctuations and entropy production in near-adiabatically driven systems. We have verified the results in a quantum chiral transport and Brownian heat pump, both analytically and numerically. This geometry framework can be readily adopted to study the effect of quantum phenomena (like quantum coherence [95–97], squeezing [98,99]) on the performance and TURs of heat engines in the finite-time regime. Also, deriving optimal protocols with minimal fluctuations under cyclic parametric driving with arbitrary speed is an important future direction.

We acknowledge the support from the National Natural Science Foundation of China (No. 11935010), the Natural Science Foundation of Shanghai (No. 23ZR1481200), the Program of Shanghai Academic Research Leader (No. 23XD1423800), and the Opening Project of Shanghai Key Laboratory of Special Artificial Microstructure Materials and Technology.

*Corresponding author: Xonics@tongji.edu.cn

[1] V. Blickle and C. Bechinger, Realization of a micrometre-sized stochastic heat engine, Nat. Phys. **8**, 143 (2012).
[2] J. Roßnagel, O. Abah, F. Schmidt-Kaler, K. Singer, and E. Lutz, Nanoscale heat engine beyond the carnot limit, Phys. Rev. Lett. **112**, 030602 (2014).
[3] I. A. Martínez, É. Roldán, L. Dinis, D. Petrov, J. M. Parrondo, and R. A. Rica, Brownian Carnot engine, Nat. Phys. **12**, 67 (2016).
[4] I. A. Martínez, A. Petrosyan, D. Guéry-Odelin, E. Trizac, and S. Ciliberto, Engineered swift equilibration of a Brownian particle, Nat. Phys. **12**, 843 (2016).
[5] M. Josefsson, A. Svilans, A. M. Burke, E. A. Hoffmann, S. Fahlvik, C. Thelander, M. Leijnse, and H. Linke, A quantum-dot heat engine operating close to the thermodynamic efficiency limits, Nat. Nanotechnol. **13**, 920 (2018).
[6] P. Talkner and P. Hänggi, Colloquium: Statistical mechanics and thermodynamics at strong coupling: Quantum and classical, Rev. Mod. Phys. **92**, 041002 (2020).
[7] R. Wang, C. Wang, J. Lu, and J.-H. Jiang, Inelastic thermoelectric transport and fluctuations in mesoscopic systems, Adv. Phys. X **7**, 2082317 (2022).
[8] T. K. Saha, J. N. Lucero, J. Ehrich, D. A. Sivak, and J. Bechhoefer, Maximizing power and velocity of an information engine, Proc. Natl. Acad. Sci. U.S.A. **118**, e2023356118 (2021).
[9] V. Holubec and A. Ryabov, Fluctuations in heat engines, J. Phys. A **55**, 013001 (2021).
[10] A. C. Barato and U. Seifert, Cost and precision of Brownian clocks, Phys. Rev. X **6**, 041053 (2016).
[11] V. Holubec and A. Ryabov, Cycling tames power fluctuations near optimum efficiency, Phys. Rev. Lett. **121**, 120601 (2018).

[12] H. J. D. Miller, M. H. Mohammady, M. Perarnau-Llobet, and G. Guarnieri, Thermodynamic uncertainty relation in slowly driven quantum heat engines, Phys. Rev. Lett. **126**, 210603 (2021).
[13] D. J. Thouless, Quantization of particle transport, Phys. Rev. B **27**, 6083 (1983).
[14] M. V. Berry, Quantal phase factors accompanying adiabatic changes, Proc. R. Soc. A **392**, 45 (1984).
[15] P. W. Brouwer, Scattering approach to parametric pumping, Phys. Rev. B **58**, R10135 (1998).
[16] N. A. Sinitsyn and I. Nemenman, Universal geometric theory of mesoscopic stochastic pumps and reversible ratchets, Phys. Rev. Lett. **99**, 220408 (2007).
[17] S. Rahav, J. Horowitz, and C. Jarzynski, Directed flow in nonadiabatic stochastic pumps, Phys. Rev. Lett. **101**, 140602 (2008).
[18] J. Ren, P. Hänggi, and B. Li, Berry-phase-induced heat pumping and its impact on the fluctuation theorem, Phys. Rev. Lett. **104**, 170601 (2010).
[19] J. Ren, S. Liu, and B. Li, Geometric heat flux for classical thermal transport in interacting open systems, Phys. Rev. Lett. **108**, 210603 (2012).
[20] T. Yuge, T. Sagawa, A. Sugita, and H. Hayakawa, Geometrical pumping in quantum transport: Quantum master equation approach, Phys. Rev. B **86**, 235308 (2012).
[21] T. Chen, X.-B. Wang, and J. Ren, Dynamic control of quantum geometric heat flux in a nonequilibrium spin-boson model, Phys. Rev. B **87**, 144303 (2013).
[22] C. Wang, J. Ren, and J. Cao, Unifying quantum heat transfer in a nonequilibrium spin-boson model with full counting statistics, Phys. Rev. A **95**, 023610 (2017).
[23] K. L. Watanabe and H. Hayakawa, Geometric fluctuation theorem for a spin-boson system, Phys. Rev. E **96**, 022118 (2017).
[24] W. Nie, G. Li, X. Li, A. Chen, Y. Lan, and S.-Y. Zhu, Berry-phase-like effect of thermo-phonon transport in optomechanics, Phys. Rev. A **102**, 043512 (2020).
[25] Z. Wang, L. Wang, J. Chen, C. Wang, and J. Ren, Geometric heat pump: Controlling thermal transport with time-dependent modulations, Front. Phys. **17**, 13201 (2022).
[26] J. Monsel, J. Schulenborg, T. Baquet, and J. Splettstoesser, Geometric energy transport and refrigeration with driven quantum dots, Phys. Rev. B **106**, 035405 (2022).
[27] Z. Wang, J. Chen, and J. Ren, Geometric heat pump and no-go restrictions of nonreciprocity in modulated thermal diffusion, Phys. Rev. E **106**, L032102 (2022).
[28] S. K. Giri and H. P. Goswami, Geometric phaselike effects in a quantum heat engine, Phys. Rev. E **96**, 052129 (2017).
[29] B. Bhandari, P. T. Alonso, F. Taddei, F. von Oppen, R. Fazio, and L. Arrachea, Geometric properties of adiabatic quantum thermal machines, Phys. Rev. B **102**, 155407 (2020).
[30] Y. Hino and H. Hayakawa, Geometrical formulation of adiabatic pumping as a heat engine, Phys. Rev. Res. **3**, 013187 (2021).
[31] H. Hayakawa, V. M. Paasonen, and R. Yoshii, Geometrical quantum chemical engine, arXiv:2112.12370.
[32] J. Ren, Geometric thermoelectric pump: Energy harvesting beyond seebeck and pyroelectric effects, Chin. Phys. Lett. **40**, 090501 (2023).
[33] K. Takahashi, K. Fujii, Y. Hino, and H. Hayakawa, Nonadiabatic control of geometric pumping, Phys. Rev. Lett. **124**, 150602 (2020).
[34] K. Funo, N. Lambert, F. Nori, and C. Flindt, Shortcuts to adiabatic pumping in classical stochastic systems, Phys. Rev. Lett. **124**, 150603 (2020).
[35] B. Andresen, P. Salamon, and R. S. Berry, Thermodynamics in finite time, Phys. Today **37**, 62 (1984).
[36] P. Salamon and R. S. Berry, Thermodynamic length and dissipated availability, Phys. Rev. Lett. **51**, 1127 (1983).
[37] G. E. Crooks, Measuring thermodynamic length, Phys. Rev. Lett. **99**, 100602 (2007).
[38] E. H. Feng and G. E. Crooks, Far-from-equilibrium measurements of thermodynamic length, Phys. Rev. E **79**, 012104 (2009).
[39] D. A. Sivak and G. E. Crooks, Thermodynamic metrics and optimal paths, Phys. Rev. Lett. **108**, 190602 (2012).
[40] E. Aurell, K. Gawedzki, C. Mejía-Monasterio, R. Mohayaee, and P. Muratore-Ginanneschi, Refined second law of thermodynamics for fast random processes, J. Stat. Phys. **147**, 487 (2012).
[41] M. Nakazato and S. Ito, Geometrical aspects of entropy production in stochastic thermodynamics based on Wasserstein distance, Phys. Rev. Res. **3**, 043093 (2021).
[42] T. Van Vu and Y. Hasegawa, Geometrical bounds of the irreversibility in Markovian systems, Phys. Rev. Lett. **126**, 010601 (2021).
[43] T. Van Vu and K. Saito, Thermodynamic unification of optimal transport: Thermodynamic uncertainty relation, minimum dissipation, and thermodynamic speed limits, Phys. Rev. X **13**, 011013 (2023).
[44] E. Aurell, C. Mejía-Monasterio, and P. Muratore-Ginanneschi, Optimal protocols and optimal transport in stochastic thermodynamics, Phys. Rev. Lett. **106**, 250601 (2011).
[45] P. Muratore-Ginanneschi, C. Mejía-Monasterio, and L. Peliti, Heat release by controlled continuous-time Markov jump processes, J. Stat. Phys. **150**, 181 (2013).
[46] P. Muratore-Ginanneschi and K. Schwieger, How nanomechanical systems can minimize dissipation, Phys. Rev. E **90**, 060102(R) (2014).
[47] G. Guarnieri, G. T. Landi, S. R. Clark, and J. Goold, Thermodynamics of precision in quantum nonequilibrium steady states, Phys. Rev. Res. **1**, 033021 (2019).
[48] K. Brandner and K. Saito, Thermodynamic geometry of microscopic heat engines, Phys. Rev. Lett. **124**, 040602 (2020).
[49] J. Eglinton and K. Brandner, Geometric bounds on the power of adiabatic thermal machines, Phys. Rev. E **105**, L052102 (2022).
[50] H. J. D. Miller, M. Scandi, J. Anders, and M. Perarnau-Llobet, Work fluctuations in slow processes: Quantum signatures and optimal control, Phys. Rev. Lett. **123**, 230603 (2019).
[51] P. Abiuso and M. Perarnau-Llobet, Optimal cycles for low-dissipation heat engines, Phys. Rev. Lett. **124**, 110606 (2020).
[52] H. J. D. Miller and M. Mehboudi, Geometry of work fluctuations versus efficiency in microscopic thermal machines, Phys. Rev. Lett. **125**, 260602 (2020).

[53] P. Abiuso, H. J. Miller, M. Perarnau-Llobet, and M. Scandi, Geometric optimisation of quantum thermodynamic processes, Entropy **22**, 1076 (2020).

[54] K. Proesmans, J. Ehrich, and J. Bechhoefer, Finite-time Landauer principle, Phys. Rev. Lett. **125**, 100602 (2020).

[55] J.-F. Chen, C. P. Sun, and H. Dong, Extrapolating the thermodynamic length with finite-time measurements, Phys. Rev. E **104**, 034117 (2021).

[56] P. Terrén Alonso, P. Abiuso, M. Perarnau-Llobet, and L. Arrachea, Geometric optimization of nonequilibrium adiabatic thermal machines and implementation in a qubit system, PRX Quantum **3**, 010326 (2022).

[57] A. G. Frim and M. R. DeWeese, Geometric bound on the efficiency of irreversible thermodynamic cycles, Phys. Rev. Lett. **128**, 230601 (2022).

[58] A. G. Frim and M. R. DeWeese, Optimal finite-time Brownian Carnot engine, Phys. Rev. E **105**, L052103 (2022).

[59] G. Li, J.-F. Chen, C. P. Sun, and H. Dong, Geodesic path for the minimal energy cost in shortcuts to isothermality, Phys. Rev. Lett. **128**, 230603 (2022).

[60] M. Scandi, D. Barker, S. Lehmann, K. A. Dick, V. F. Maisi, and M. Perarnau-Llobet, Minimally dissipative information erasure in a quantum dot via thermodynamic length, Phys. Rev. Lett. **129**, 270601 (2022).

[61] P. Abiuso, V. Holubec, J. Anders, Z. Ye, F. Cerisola, and M. Perarnau-Llobet, Thermodynamics and optimal protocols of multidimensional quadratic brownian systems, J. Phys. Commun. **6**, 063001 (2022).

[62] S. Dago and L. Bellon, Dynamics of information erasure and extension of Landauer's bound to fast processes, Phys. Rev. Lett. **128**, 070604 (2022).

[63] A. C. Barato and U. Seifert, Thermodynamic uncertainty relation for biomolecular processes, Phys. Rev. Lett. **114**, 158101 (2015).

[64] T. R. Gingrich, J. M. Horowitz, N. Perunov, and J. L. England, Dissipation bounds all steady-state current fluctuations, Phys. Rev. Lett. **116**, 120601 (2016).

[65] T. R. Gingrich, G. M. Rotskoff, and J. M. Horowitz, Inferring dissipation from current fluctuations, J. Phys. A **50**, 184004 (2017).

[66] S. Pal, S. Saryal, D. Segal, T. S. Mahesh, and B. K. Agarwalla, Experimental study of the thermodynamic uncertainty relation, Phys. Rev. Res. **2**, 022044(R) (2020).

[67] C. Yang, X. Wei, J. Sheng, and H. Wu, Phonon heat transport in cavity-mediated optomechanical nanoresonators, Nat. Commun. **11**, 4656 (2020).

[68] P. Pietzonka, F. Ritort, and U. Seifert, Finite-time generalization of the thermodynamic uncertainty relation, Phys. Rev. E **96**, 012101 (2017).

[69] K. Liu, Z. Gong, and M. Ueda, Thermodynamic uncertainty relation for arbitrary initial states, Phys. Rev. Lett. **125**, 140602 (2020).

[70] S. Saryal and B. K. Agarwalla, Bounds on fluctuations for finite-time quantum Otto cycle, Phys. Rev. E **103**, L060103 (2021).

[71] Y. Hasegawa, Quantum thermodynamic uncertainty relation for continuous measurement, Phys. Rev. Lett. **125**, 050601 (2020).

[72] Y. Hasegawa, Thermodynamic uncertainty relation for general open quantum systems, Phys. Rev. Lett. **126**, 010602 (2021).

[73] T. Van Vu and K. Saito, Thermodynamics of precision in Markovian open quantum dynamics, Phys. Rev. Lett. **128**, 140602 (2022).

[74] K. Macieszczak, K. Brandner, and J. P. Garrahan, Unified thermodynamic uncertainty relations in linear response, Phys. Rev. Lett. **121**, 130601 (2018).

[75] K. Proesmans and J. M. Horowitz, Hysteretic thermodynamic uncertainty relation for systems with broken time-reversal symmetry, J. Stat. Mech. 054005 (2019).

[76] P. P. Potts and P. Samuelsson, Thermodynamic uncertainty relations including measurement and feedback, Phys. Rev. E **100**, 052137 (2019).

[77] M. Esposito, U. Harbola, and S. Mukamel, Nonequilibrium fluctuations, fluctuation theorems, and counting statistics in quantum systems, Rev. Mod. Phys. **81**, 1665 (2009).

[78] M. Campisi, P. Hänggi, and P. Talkner, Colloquium: Quantum fluctuation relations: Foundations and applications, Rev. Mod. Phys. **83**, 771 (2011).

[79] Y. Hasegawa and T. Van Vu, Fluctuation theorem uncertainty relation, Phys. Rev. Lett. **123**, 110602 (2019).

[80] J. M. Horowitz and T. R. Gingrich, Thermodynamic uncertainty relations constrain non-equilibrium fluctuations, Nat. Phys. **16**, 15 (2020).

[81] U. Seifert, From stochastic thermodynamics to thermodynamic inference, Annu. Rev. Condens. Matter Phys. **10**, 171 (2019).

[82] Z. Cao, J. Su, H. Jiang, and Z. Hou, Effective entropy production and thermodynamic uncertainty relation of active Brownian particles, Phys. Fluids **34**, 053310 (2022).

[83] Z. Cao and Z. Hou, Improved estimation for energy dissipation in biochemical oscillations, J. Chem. Phys. **157**, 025102 (2022).

[84] T. Koyuk, U. Seifert, and P. Pietzonka, A generalization of the thermodynamic uncertainty relation to periodically driven systems, J. Phys. A **52**, 02LT02 (2018).

[85] T. Koyuk and U. Seifert, Operationally accessible bounds on fluctuations and entropy production in periodically driven systems, Phys. Rev. Lett. **122**, 230601 (2019).

[86] T. Koyuk and U. Seifert, Thermodynamic uncertainty relation for time-dependent driving, Phys. Rev. Lett. **125**, 260604 (2020).

[87] C. Maes, Frenesy: Time-symmetric dynamical activity in nonequilibria, Phys. Rep. **850**, 1 (2020).

[88] See Supplemental Material at http://link.aps.org/supplemental/10.1103/PhysRevLett.132.207101 for details, which includes Refs. [19,37,48,65,69,86,89].

[89] A. Dechant and S.-i. Sasa, Fluctuation–response inequality out of equilibrium, Proc. Natl. Acad. Sci. U.S.A. **117**, 6430 (2020).

[90] Y. Aharonov and J. Anandan, Phase change during a cyclic quantum evolution, Phys. Rev. Lett. **58**, 1593 (1987).

[91] J. Lu, Z. Wang, J. Peng, C. Wang, J.-H. Jiang, and J. Ren, Geometric thermodynamic uncertainty relation in a periodically driven thermoelectric heat engine, Phys. Rev. B **105**, 115428 (2022).

[92] R. D. Astumian and P. Hänggi, Brownian motors, Phys. Today **55**, No. 11, 33 (2002).
[93] R. Kosloff and A. Levy, Quantum heat engines and refrigerators: Continuous devices, Annu. Rev. Phys. Chem. **65**, 365 (2014).
[94] V. Y. Chernyak and N. A. Sinitsyn, Pumping restriction theorem for stochastic networks, Phys. Rev. Lett. **101**, 160601 (2008).
[95] K. Brandner, M. Bauer, and U. Seifert, Universal coherence-induced power losses of quantum heat engines in linear response, Phys. Rev. Lett. **119**, 170602 (2017).
[96] K. Ptaszyński, Coherence-enhanced constancy of a quantum thermoelectric generator, Phys. Rev. B **98**, 085425 (2018).
[97] P. A. Camati, J. F. G. Santos, and R. M. Serra, Coherence effects in the performance of the quantum Otto heat engine, Phys. Rev. A **99**, 062103 (2019).
[98] G. Schaller, *Open Quantum Systems Far from Equilibrium* (Springer, New York, 2014), Vol. 881.
[99] C. Wang, H. Chen, and J.-Q. Liao, Nonequilibrium thermal transport and photon squeezing in a quadratic qubit-resonator system, Phys. Rev. A **104**, 033701 (2021).